VERTICAL PROFILE WEIGHTING OF METEOROLOGICAL EFFECTS ON SOUND PROPAGATION

S von Hünerbein University of Salford, Acoustic Research Center, Salford
SG Bradley University of Salford, Acoustic Research Center, Salford

1. INTRODUCTION

This paper examines the relationship between meteorological variations and the sound intensity recorded at various distances from a surface-based source. Specifically, we are concerned with the relative significance of meteorological fluctuations at various heights, as a function of distance between acoustic source and receiver. The objectives relate to both the *forward problem* (determination of the sound field in the presence of variable meteorology), and to the *inverse problem* (determination of the meteorology from the sound field) and aim to

- Provide guidelines for field experiment design involving meteorological profiles
- Provide guidelines for propagation model design
- Determine feasibility of acoustic tomography of the atmospheric boundary layer.

The first of these objectives is driven by the observation that acoustic propagation experimentalists are generally not well-informed on meteorology. The second objective addresses the fact that, historically, propagation models employ very simplistic, but fast, similarity codes to describe the atmospheric boundary layer. More recently, comprehensive atmospheric mesoscale models have been used, but these are slow and memory-intensive. Consequently, a need is identified to match the design of a meteorological model to the requirements of acoustic propagation simulation. The third objective arises from the increasing interest in atmospheric acoustic tomography (Bradley et al., 2002).

2. VERTICAL PROFILE WEIGHTING

We consider, for simplicity, the two-dimensional case of intensity $I(R)$ being recorded at range R from an omni-directional source. The intervening atmosphere, at horizontal distance x and vertical distance z from the source, is characterized by sound speed $c(x,z)$ and turbulent scattering, which are functions of other scalars. In general the receiver and source are elevated and surface impedance effects need to be included. However, neglecting these parameters and considering receiver and source based on an absorbing surface will have little influence on the dependence of I on the meteorology above the source-receiver line. We therefore write

$$I(R) = S\int_0^R \left[\int_0^\infty \mathbf{w} \bullet \nabla \zeta \, dz\right] dx \qquad (1)$$

where S includes source strength, ζ is some scalar (such as temperature) affecting sound intensity, and $\boldsymbol{w}$ is a weighting kernel. For a plane-parallel atmosphere, $\zeta(x,z) = \zeta(z)$ and (1) becomes

$$I(R) = S\int_0^\infty w(R,z)\frac{d\zeta(z)}{dz} dz \qquad (2)$$

In practice a discrete form is used for M measurements y_i, i=1,2,....M and N heights z_j, j=1,2,....N

$$y_i = \sum_{j=1}^{N} w_{ij}\,\phi_j \tag{3}$$

where w_{ij} are weights, and ϕ_j atmospheric gradients, at each height z_j. The gradients carry the meteorological field information. Of interest is the variation in recorded intensity for variations in scalar gradient at each height. From (3),

$$\sigma_{y_i}^2 = \sum_{j=1}^{N} w_{ij}^2\,\sigma_{\phi_j}^2 \tag{4}$$

For the forward problem, it would be useful to extract some simpler measure of the vertical weighting, such as z_n, the height below which fraction γ of the variance is accounted for:

$$\gamma\sigma_{y_i}^2 = \sum_{j=1}^{n} w_{ij}^2\,\sigma_{\phi_j}^2 \tag{5}$$

For the inverse problem, constrained linear inversion is used to find ϕ_j. The vertical distribution of the w_{ij}, and the measurement errors, determine the quality of the retrievals.

3. EVALUATION OF WEIGHTING FUNCTIONS

Two methods are used to evaluate ***w***. The first is a meteorological model, which provides a range of meteorology. The second is use of actual field data, but from a restricted data set. Each of these sources of meteorological profiles can be used in a new propagation model which includes turbulent scattering.

3.1 Turbulent scattering

The effect of turbulent scattering on sound propagation is of intense current interest. Most effort is being directed toward obtaining good statistical descriptions of the scattering cross section (e.g. Ostashev et al., 1999) and bringing together the atmospheric science and acoustic literatures (Wilson et al., 1999). Estimation of the relative contributions of temperature and velocity *turbulent fluctuations* has been considered by Ostashev and Wilson (2000). The approach taken here is based on the original Tatarski (1971) work.

Turbulent scattering occurs from incoherent fluctuations having scales χ from the inner scale λ_i (~0.01m) to the outer scale L_o (~100m). For smaller scales the scattering is negligible, whereas for larger scales the structures tend to be coherent and not treatable by statistical theories. Scattering is very strongly associated with acoustic wavenumber

$$k = \frac{1}{\chi\sqrt{2(1-\mu)}} \tag{6}$$

where μ is the cosine of the scattering angle (angle between forward direction and scattering direction). Turbulence theory gives for the scattering cross-section per unit volume of air, when scattering is into solid angle $d\Omega$, as

$$\sigma_s d\Omega = \frac{1}{8} k^{\frac{1}{3}} \frac{\mu^2}{[2(1-\mu)]^{\frac{11}{6}}} \left[\Gamma_T + (1+\mu)\Gamma_V\right] d\Omega \tag{7a}$$

where

$$\Gamma_T = 0.033\frac{C_T^2}{T^2} \tag{7b}$$

and

$$\Gamma_V = 0.76\frac{C_V^2}{2\pi c^2}. \tag{7c}$$

Here C_T^2 and C_V^2 are measures of the strength of temperature T and velocity V fluctuations and are obtained from time averages over spatially-separated measurements

$$C_T^2 = \left\langle [T(x+\Delta x)-T(x)]^2 \right\rangle (\Delta x)^{-\frac{2}{3}}$$
$$C_V^2 = \left\langle [V(x+\Delta x)-V(x)]^2 \right\rangle (\Delta x)^{-\frac{2}{3}}. \tag{8}$$

In path length s, scattering reduces the acoustic intensity from I_o to

$$I = I_o e^{-k_s s} \tag{9}$$

where

$$k_s = \oint \sigma_s d\Omega = 2\pi \int_{-1}^{1-\delta} \sigma_s d\mu \tag{10}$$

and

$$\delta = \frac{1}{2k^2 L_o^2}. \tag{11}$$

We make use of the following integral

$$\Phi(\mu_s) = \frac{5\delta^{\frac{5}{6}}}{6(\Gamma_T+\Gamma_V)} \int_{\mu_s}^{1-\delta} \frac{[\Gamma_T+(1+\mu)\Gamma_V]}{(1-\mu)^{\frac{11}{6}}} \mu^2 d\mu$$
$$= 1-$$
$$\frac{5}{(\Gamma_T+\Gamma_V)}\left[\frac{1}{5}(\Gamma_T+\Gamma_V)\eta^{-\frac{5}{6}} + (2\Gamma_T+3\Gamma_V)\eta^{\frac{1}{6}} - \frac{1}{7}(\Gamma_T+3\Gamma_V)\eta^{\frac{7}{6}} - \frac{1}{13}\Gamma_V\eta^{\frac{13}{6}}\right]\delta^{\frac{5}{6}} +$$
$$\frac{5}{(\Gamma_T+\Gamma_V)}\left[(2\Gamma_T+3\Gamma_V)\delta - \frac{1}{7}(\Gamma_T+3\Gamma_V)\delta^2 - \frac{1}{13}\Gamma_V\delta^3\right] \tag{12}$$

where

$$\eta = 1-\mu_s.$$

Then

$$k_s = \frac{3\pi}{20}k^2 L_o^{\frac{5}{3}}(\Gamma_T+\Gamma_V)\Phi(-1). \tag{13}$$

3.2 Propagation model

Scattering by turbulence can be treated via analogy to the raft of methods for solution to the Radiative Transfer Equation used to model optical propagation in complex situations. We call these new models ARTEA (Acoustic Radiative Transfer Equation

Analog). Here we use a Monte Carlo ray-tracing code with random deviations based on the probability of scattering in each direction (c.f. Bradley et al., 2000). A ray is initiated from the source at a particular zenith angle and advanced by steps down the range. Refraction is included at each step and absorption is based on Neff(1975). For each step, the probability of scatter is

$$1-e^{-k_s \Delta s}$$

and, if scattering occurs, the probability of scattering into solid angle $d\Omega$ is

$$\frac{\sigma_s d\Omega}{k_s} .$$

These probabilities are used to select a new ray direction at each step, until a ray reaches the surface, at which time its position and zenith angle are recorded. Although in reality scattering is a continuous process like absorption, the Monte Carlo method allocates appropriate weighting to scattering according to the scattering pattern represented by the scattering cross section.

The selection method is to generate, at each step, a random uniform variate, U_1, and scatter if

$$1-e^{-k_s \Delta s} > U_1 .$$

If scattering occurs, the scattering angle is based on a scattering phase function $p(\mu)$ which is proportional to σ_s but normalized via

$$\frac{1}{2}\int_{-1}^{1-\delta} p(\mu)d\mu = 1 . \qquad (14)$$

This gives

$$p(\mu) = \frac{\pi}{2k_s} k^{\frac{1}{3}} \frac{\mu^2}{[2(1-\mu)]^{\frac{11}{6}}} \left[\Gamma_T + (1+\mu)\Gamma_V\right] . \qquad (15)$$

A typical scattering phase function is shown in Fig. 1.

The rejection method is used to find the scattering angle. A second uniform random deviate U_2 is chosen, and μ_s found from

$$\frac{1}{2}\int_{\mu_s}^{1-\delta} p(\mu)d\mu = \frac{\Phi(\mu_s)}{\Phi(-1)} = U_2 . \qquad (16)$$

Equation (16) may be solved efficiently by iteration, since $\eta \approx \delta$. Once the scattered ray direction is found, the process is repeated.

3.3 Meteorological model

In addition to the three turbulence parameters (L_o, C_T^2, and C_V^2), refraction and absorption require fields for wind speed V, temperature T, and humidity mixing ratio q. Profiles of these seven parameters are provided from a one-dimensional boundary-layer model. This model is an adaptation of the time-dependent Penn State model described by Blackadar(). It has 30 atmospheric layers with the lowest layer 10m thick and the top layer extending to 3km. Surface vegetation and soil features are included, as well as cloud development, turbulence, and radiative transfer. The model is initialized with field observations of potential temperature θ, V, and q, and its output includes time-varying profiles of gradient Richardson number R_i, and eddy diffusivity K, from which we derive

$$C_T^2 = 3.21\left(\frac{\theta K^2}{g}\right)^{\frac{1}{3}}\left(\frac{\partial\theta}{\partial z}\right)^{\frac{5}{3}}\left(\frac{1}{P_r^2}\frac{R_i}{P_r - R_i}\right)^{\frac{1}{3}} \quad (17a)$$

and

$$C_V^2 = \frac{C_T^2}{1.63\dfrac{R_i}{P_r - R_i}\dfrac{\theta}{g}\dfrac{\partial\theta}{\partial z}}. \quad (17b)$$

3.4 Weighting function estimation

The integrated acoustic-meteorological model is run without perturbations to the model-generated atmospheric profiles, and then again at each of the *N* heights with a small perturbation of the scalar at that height. Then

$$w_{ij} = \frac{\partial y_i}{\partial \phi_j}. \quad (18)$$

In practice we plot variation in dB for variations in temperature, wind speed, C_T^2, and C_V^2.

4. Example results

Figure 2 shows a temperature and wind speed profile from the model run initialized from Blackadar's Great Plains Field Experiment dataset. The model produces output at 30 vertical levels, but this has been extended by spline interpolation to provide 30 levels below 1km. This profile is characterized by a strong inversion at 400m extending through another 100m. The upper inversion at 2500m is not significant for propagation over the 10 km range considered. The wind profile shows a weak jet with peak speed at about 1500m. The net result is a limited cone of down-bending sound extending out to the 10km edge of the model domain. Surface intensity initially falls off slightly faster than inverse-square, but then becomes more complex after 2.5km range.

The weighting function for temperature sensitivity is shown in Fig. 3 and that for wind speed sensitivity in Fig.4. Since this paper is concerned with the weighting-function methodology, here we will not attempt detailed interpretation. The most significant finding is, for this atmospheric profile, that all dependency on meteorology is essentially confined below 300m. Secondly, both sets of weighting functions show regions where increase of temperature or wind cause an increase in sound intensity, and other regions, more elevated, where the converse is true. This is no doubt related to the sound speed profile and to whether extra curvature is introduced lower down or near the apex of a ray path.

5. Discussion

This paper introduces a method for investigating the sensitivity of sound propagation to complex meteorology. The work is ongoing and further details will be available from a fuller paper to be submitted to JASA. In particular, the weighting functions for the turbulent scattering are not shown in the current paper.

Some important findings are that, for the case presented,

- Meteorology in the lowest 300m is significant
- Surface (i.e. 10m) meteorology measurements are demonstrably inadequate

- SODAR / LIDAR measurements ranging to 200-400m height give useful data
- Elevated (200m) meteorological variability can be more important than the surface

Finally, it is of interest that the weighting functions show considerable structure for this case study. This suggests that acoustic tomography, in which the scalars are to be found from inverting Eqn. (3), has some potential.

2002 Bradley, S. G., S. von Hünerbein, and A. Haddad. Atmospheric acoustic interferometer tomography of temperature and winds. *Accepted by Acustica.*

2000 Bradley, S. G., C. D. Stow, C. A. Lynch-Blosse. Measurements of Rainfall Properties Using Long Optical Path Imaging. *J. Atmos. Oceanic Technol.* **17**, 761–772.

1975 Neff, W. D., Quantitative evaluation of acoustic echoes from the planetary boundary layer, *U.S. Dept. of Commerce NOAA TR ERL 322-WPL 38.* 34pp.

2000 Ostashev, V. E. and D. K. Wilson. Relative contributions from temperature and wind velocity fluctuations to the statistical moments of a sound field in a turbulent atmosphere. *Acustica*, **86**, 260-268.

1999 Ostashev, V. E., G. H. Goedecke, R. Wood, H. Auvermann, and S. F. Clifford. Sound scattering cross-section in a stratified moving atmosphere. *J. Acoust. Soc. Am.*, **105**, 3115-3125.

1971 Tatarski, V. I., The effects of the turbulent atmosphere on wave propagation. Keter, Jerusalem.

1999 Wilson, D. K., J. G. Brasseaur, and K. E. Gilbert. Acoustic scattering and the spectrum of atmospheric turbulence. *J.A.S.A.*, **105**, 30-34.

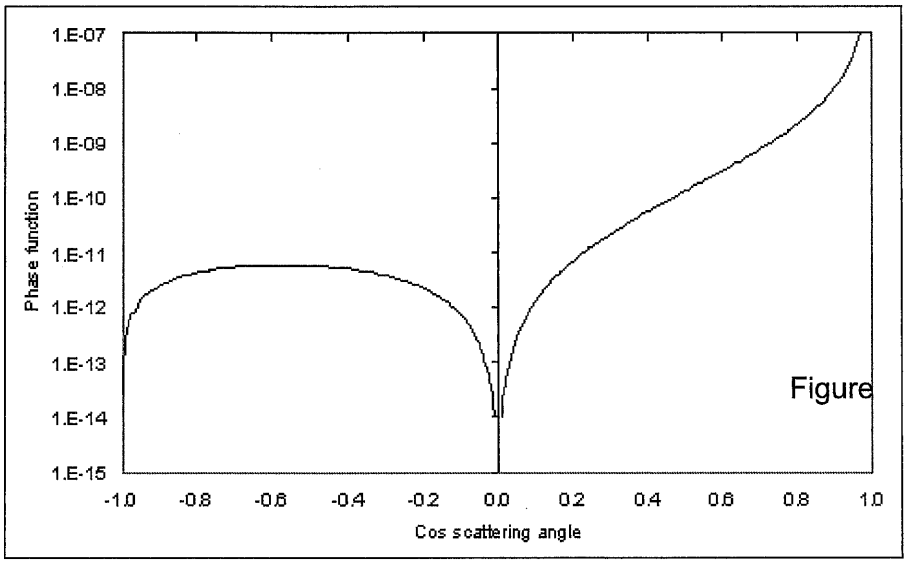

Figure 1. Turbulent scattering phase function for L0=100 m, $C_T^2=10^{-5}$ $m^{-2/3}$, and $C_V^2=0.01$.

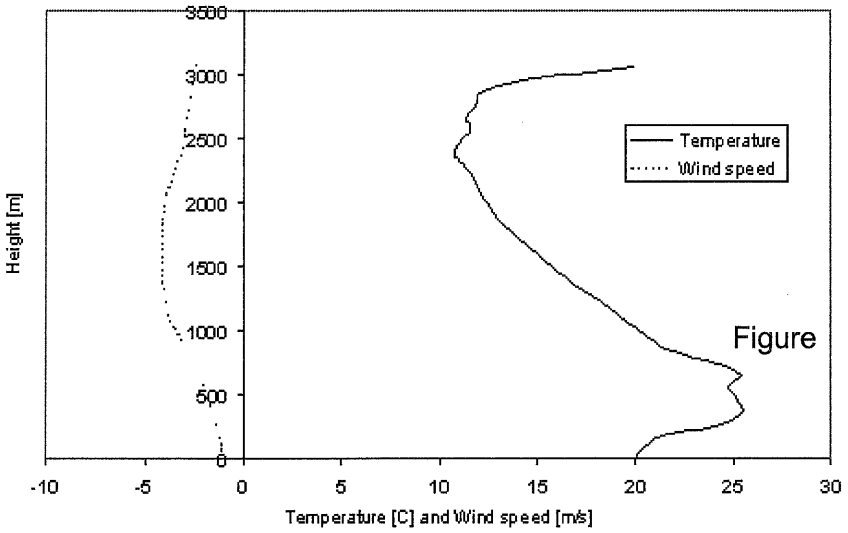

Figure 2. Atmospheric profiles of temperature and wind speed for the case study.

Figure 3. Weighting functions for temperature sensitivity.

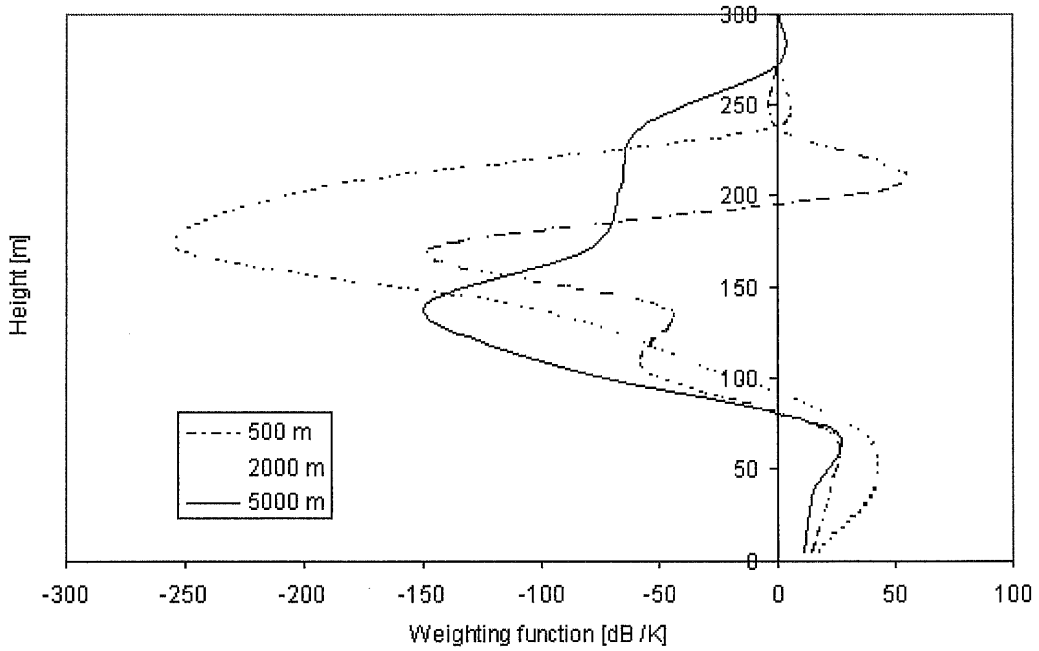

Figure 4. Weighting functions for wind-speed sensitivity.

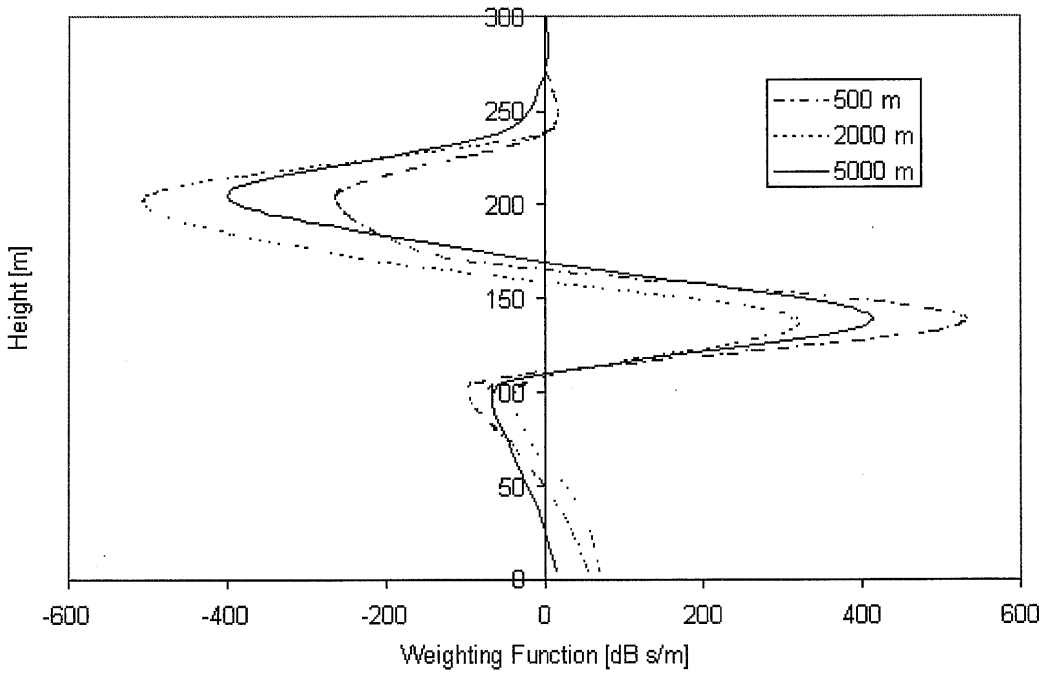
300
250
200
150
100
50
0
Height [m]
500 m
2000 m
5000 m
-600
-400
-200
0
200
400
600
Weighting Function [dB s/m]